X-611-67-217

NASA TM X- 55810

HIGHER ORDER RING CURRENTS AND PARTICLE ENERGY STORAGE IN THE MAGNETOSPHERE

MAY 1967

GPO PRICE $ _____

CFSTI PRICE(S) $ _____

Hard copy (HC) 3.00

Microfiche (MF) .65

ff 653 July 65

GODDARD SPACE FLIGHT CENTER

GREENBELT, MARYLAND

X-611-67-217

HIGHER ORDER RING CURRENTS AND PARTICLE ENERGY STORAGE IN THE MAGNETOSPHERE

R. A. Hoffman
P. A. Bracken

May 1967

Goddard Space Flight Center
Greenbelt, Maryland

Higher Order Ring Currents and Particle Energy Storage in the Magnetosphere

by

R. A. Hoffman and P. A. Bracken

NASA Goddard Space Flight Center
Greenbelt, Maryland

Abstract

A system of cumputer programs has been developed to calculate by successive approximations the ring current magnetic field to any order from an arbitrarily defined distribution of particles in any field model.

Using a field model containing the boundary and neutral sheet fields in addition to the main field, third order ring current fields have been calculated for various enhancements of a reasonable particle distribution model. A number of properties of high intensity ring currents have been investigated including the following. (1) Diamagnetism alone poorly describes the field deformation in the heart of the ring current region. (2) In spite of the inclusion of particle energy densities reaching twice the ambient field energy density, the total magnetic field is not inordinately distorted. Self-consistent solutions are easily obtained, and a null point in the field appears difficult to reach. (3) The ratio of particle energy density to final field energy density, β, has been considered. It is shown that very large particle energy densities will not themselves provide the limitation on β by obliterating the field. Therefore, it is required of dynamic mechanisms to quantitatively place the upper limits on β.

HIGHER ORDER RING CURRENTS AND PARTICLE ENERGY STORAGE IN THE MAGNETOSPHERE

INTRODUCTION:

The problem of calculating the magnetic effects of a distribution of charged particles trapped in the magnetosphere is made difficult by the fact that the particles move in a magnetic field, a portion of which is due to the particle motion itself. Since the precise distribution of currents produced by the motions of the particles are directly related to the total magnetic field configuration in which they move, and the magnetic effects at the location of the particles must be calculated from the current distributions, there is no simple way of obtaining an exact solution to the problem. (See Akasofu, 1963, for a review of the ring current problem.)

One way of investigating this interconnection between the trapped particles and their fields is by successive approximations to the true field (Akasofu and Chapman, 1961). This is accomplished in the following manner: the electric current distribution is first calculated from a given particle distribution, p, moving in a magnetic field configuration, $\vec{B}$, composed of fields from the earth's internal currents, the boundary currents and neutral sheet currents:

$$\vec{i} = f(\vec{B}, p)$$

From this current distribution, a first order ring current field is calculated:

$$\vec{\Delta B}(1) = F(\vec{i})$$

from the Biot-Savart law. This ring current field is then included in the magnetic field configuration, from which a new $\vec{i}$ is determined, and then a new $\vec{\Delta B}(2)$. The cycle is continued by recalculating the current distribution for the n^{th} time for the particles moving in a field configuration containing the ring current field calculated from the previous cycle, $n - 1$. When $\vec{\Delta B}(n) = \vec{\Delta B}(n - 1)$, a self consistent solution has been obtained. Unfortunately this method requires a considerable amount of numerical calculations, which only becomes feasible with a computer, and has been performed only once to the second order for a very special field and particle distribution (Akasofu, Cain and Chapman, 1961).

In order to more simply estimate the magnetic effects of a particle distribution, several approximate approaches have been adopted. Most used is the expression for a plasma confined in an infinitely long cylinder with external magnetic field lines parallel to the axis of the cylinder

$$p_n + p_m = p_n + \frac{B^2}{8\pi} = \frac{B_0^2}{8\pi} \qquad (1)$$

where B_0 is the field neglecting the current from the plasma.

The relationship given in (1) has been applied quite extensively to trapped particle problems. It indicates that the pressure, or energy density of the plasma, cannot exceed the energy density of the ambient field. In fact the limit

on particle energy density has usually been considered to be a small fraction of the original field energy density (Van Allen, 1966). Until very recently the maximum ratio of energy densities measured in the ring current region (out to about 6 R_E) had been about 15% and was due to protons with energies above 100 KeV (Davis and Williamson, 1963; Frank, 1967a). Now Frank (1967b) has reported on observations of protons and electrons in the tens of KeV region during magnetic disturbances whose energy densities are comparable to that of the field.

The implications of Eq. (1) were originally applied to experimental results by Dessler (1960) as one argument against the large fluxes of electrons implied by interpreting thick walled Geiger counter and ion chamber counting rates as due to bremsstrahlung from electrons of energies of the order of 30 KeV. More recently Frank (1966) has used this energy density argument to rule out protons as the source of large energy fluxes observed by a cadmium sulfide crystal detector aboard Explorer XII during a magnetic storm, and concluded that the fluxes were due to electrons in the energy range 100 ev to 40 KeV.

However, for the purpose of definitive ring current studies, we have developed a system of computer programs to calculate by successive approximations the magnetic field from an arbitrarily defined distribution of particles in any field model. With these programs it has been possible to determine the true effects of various particle energy density distributions on the magnetic field

configuration, to check the accuracy of the approximate approaches to the ring current problem, and to investigate the energy storage capabilities of the magnetosphere.

CURRENT EQUATIONS

For the calculation of the electric current distribution in the magnetosphere, we have, as in previous work (Akasofu and Chapman, 1961; Hoffman and Bracken, 1965), utilized the expressions derived by Parker (1957, equations 19 and 21) for the volume current densities arising from the gyration and drift motions of charged particles in a magnetic field. Parker's approach requires the assumptions that the particles are nonrelativistic, the guiding center approximation is valid, and there are no collisions. We further here limit the discussion to the steady-state case, with no electric fields. Therefore our basic current equation is

$$\vec{i} = \frac{c}{8\pi p_m} \vec{B} \times \left\{ \nabla p_n + \frac{(p_s - p_n)}{p_m} (\vec{B} \cdot \nabla) \frac{\vec{B}}{8\pi} \right\} \qquad (2)$$

A spherical coordinate system (r, θ, ϕ) whose axis is parallel to the earth's dipole axis will be used. (However, the earth's field will not be approximated by a dipole). We make the further simplifying assumptions that magnetic meridian planes are all parallel (any ϕ component of $\vec{B}$ is ignored) and the particle distribution is symmetric about the axis.

In detail the current equation to be evaluated then becomes

$$\vec{i} = \hat{\phi}\,\frac{c}{B^2}\left\{\left[\frac{B_r}{r}\,\frac{\partial p_n}{\partial \theta} - B_\theta\,\frac{\partial p_n}{\partial r}\right] + \frac{(p_s - p_n)}{B^2}\left[B_r^2\,\frac{\partial B_\theta}{\partial r}\right.\right. \tag{3}$$

$$\left.\left. + B_r B_\theta\left(\frac{1}{r}\,\frac{\partial B_\theta}{\partial \theta} - \frac{\partial B_r}{\partial r}\right) - \frac{B_\theta^2}{r}\,\frac{\partial B_r}{\partial \theta}\right]\right\}$$

For the evaluation one is required to produce maps in the r, θ grid of the following quantities: B, B_r, B_θ, p_s and p_n so that the partial derivatives in the r and θ directions can be determined numerically. The field magnitude and components can easily be obtained from various mathematical models of the magnetosphere, and can contain a multi-term expansion of the main field (e.g. Cain et al, 1965) as well as the effects of the boundary (e.g. Mead, 1964) and neutral sheet. From such a basic field model one then includes the ring current as a perturbation on the field configuration.

The determination of the partial pressures in every cell of the r, θ map is not so straight-forward. It is perhaps simplest to have a particle distribution defined along the magnetic equator in terms of distance and equatorial pitch angle. To obtain p_n and p_s in a cell it is necessary to first follow the field line passing through the cell to the equator (Mead, 1964). Then from the particle pitch angle distribution at that point on the equator and the relative field values

at the equator and cell it is possible to compute the pressures utilizing the first invariant

$$\frac{\sin^2 \alpha_c}{B_c} = \frac{\sin^2 \alpha_e}{B_e} \tag{4}$$

where the subscripts c and e refer to the cell and equatorial values respectively. In terms of experimental requirements the acquisition of such a complete set of particle data dictates a very low latitude satellite orbit.

MAGNETIC FIELD EQUATIONS

The magnetic field at a point R, θ (latitude) due to the ring current is denoted by its components B_p and B_z, respectively perpendicular and parallel to the dipole axis. The ring current region is then divided into elements dS specified by R', θ'. Then (Stratton, 1941)

$$B_p = -\frac{2}{ac R \cos\theta} \iint (R\sin\theta - R'\sin\theta')\left[E(k^2) - K(k^2) + (2R \cdot R'\cos\theta\cos\theta') \cdot \frac{E(k^2)}{F_-^2}\right]\frac{i}{F}\, dS \tag{5}$$

$$B_z = -\frac{2}{ac}\iint\left[K(k^2) - E(k^2) + 2R'\cos\theta'(R'\cos\theta' - R\cos\theta)\,\frac{E(k^2)}{F_-^2}\right]\frac{i}{F}\, dS$$

Here $K(k^2)$ and $E(k^2)$ denote the complete elliptic integrals of the first and second kind, respectively, and

$$K^2 = \frac{4R \cdot R' \cos\theta \cos\theta'}{F^2}$$

$$F^2 = R^2 + R'^2 + 2R \cdot R' \cos(\theta + \theta')$$

$$F_-^2 = R^2 + R'^2 - 2R \cdot R' \cos(\theta - \theta')$$

An element of cross-sectional area of the ring current region in a meridian plane is

$$dS = a^2 R' dR' d\theta$$

PARTICLE DISTRIBUTION AND FIELD MODEL

For the purpose of illustration, the following particle distribution model has been chosen:

The pitch angle distribution in number density is given by the form

$$F(R, s, \alpha) = C_\gamma \left(\frac{B_e}{B}\right)^{\gamma/2} \sin^\gamma \alpha \qquad (6)$$

The quantity $F(R, s, \alpha)$ is also differential in azimuth in contrast to Parker's definition (Parker, 1957). Although a single value of α will be assumed, no loss in generality occurs because $F(R, s, \alpha)$ may be redefined as a series of positive

integral powers in sin α (Sckopke, 1966), and our $F(R, s, \alpha)$ is merely one term of the series which contributes a partial current. However, in the following work the value of α is taken as 2.5 instead of an integral value.

Through Eq. (6) the partial pressure p_n is related to the energy density at the magnetic equator due to the normal component of the velocity vector, ξ_n (the normal energy density), by the relation

$$p_n = \xi_n (s = 0) \cdot \left(\frac{B_e}{B}\right)^{\gamma/2} \tag{7}$$

Also $p_s = \frac{2}{\gamma+2} p_n$, so the ratio of partial pressures is constant throughout the magnetosphere for α independent of distance. Therefore, the acquisition of the map of partial pressures in r, θ space requires merely the tracing of the field line from each cell to the magnetic equator to obtain B_e and $\xi_n (s = 0)$, which is only a function of range at the equator.

For the equatorial profile of ξ_n we take first the following model: ξ_n (R) is given as a parabola with a maximum value at 3.5 R_E and a half width of 1 R_E. Attached smoothly to this in terms of both value as well as slope is a tail extending to R_E of 8, whose ratio to the magnetic energy density of a dipole is a constant, (40%).

Thus for $2.086 < R_E < 4.272$

$$\xi_n = -1.831 \times 10^{-7} (R^2 - 7R + 10.25) \frac{ergs}{cm^3}$$

and for $4.272 < R_E < 8$

$$\xi_n = 1.56 \times 10^{-3} / R^6 \frac{ergs}{cm^3} \qquad (8)$$

The current in a cell whose field line traces to an equatorial value outside of these ranges, is set equal to zero. Also, the current region has been limited in latitude by ignoring all currents at latitudes larger than ±32°.

In addition to this model for ξ_n, the energy density profile of Eq. (8) has been enhanced by constant factors to determine the field distortions as a function of relative energy densities of particles. The enhancement factors (F) which multiply the Eq. (8) are given in Table I, along with the constant ratio K (in percent) of ξ_n to the dipole field energy density (ξ_d) in the region beyond 4.272 earth radii. Thus the specific particle models will be designated by ξ_n (K).

For all of the work performed in this study, the field model used is that of Cain et al (1965) (Coefficients from Hendricks and Cain 1966) plus the effects of the boundary and neutral sheet as described by Mead (1964) and Williams and Mead (1965), with the current sheet parameters as follows: front edge, $8R_E$; rear edge, $200\ R_E$; field strength adjacent to sheet, 16 γ (D. J. Williams, private communication). This field model will hereafter be referred to as the Jensen

and Cain plus Mead model. The calculations have been performed on the magnetic meridian plane at 72° E magnetic longitude at a sun-earth-plane angle of 0°, so they pertain to the sunward side of the magnetosphere only.

The normal energy density ξ_n (70%) as a function of range at the equator is plotted in Fig. 1. There also appears the ratio of ξ_n to the energy density of a dipole field, (labeled "Dipole Ratio"), which displays the constant ratio beyond a range of $4.272R_E$. However, the ratio of particle energy density to the field energy density of the Jensen and Cain plus Mead field model does not remain constant, as shown with the curve labeled "1st Ratio".

HIGHER ORDER FIELD CALCULATIONS

Figures 2 and 3 contain ΔB as a function of distance for 0° latitude. First and third order calculations of ΔB are displayed for the two cases of K = 70% and 140% (and the second order results at the maximum of ΔB for K = 140%) as well as a comparison with the first order perturbation calculated for a dipole model of the earth's field. It is noted that the second and the third order calculations decrease the perturbation profile over the first order. This higher order effect is in the opposite sense to that derived by Akasofu et al (1961b) in their second order calculation. The difference between their second and first order profiles is perhaps similar to comparing the third order and first order dipole profiles of Fig. 2, which would also show an increase. From a comparison of the first, second and third order calculations, it is expected that carrying the

procedure to the fourth order would introduce less than a one percent change on the third order.

TOTAL RING CURRENT FIELD AND DIAMAGNETISM

The relative contribution of diamagnetism to the total ring current field is first investigated.

From Eq. (1)

$$\Delta B(1) = B_0 - B = B_0 \left[1 - \sqrt{1 - \frac{\xi_n}{\xi_{of}}} \right] \tag{9}$$

where $\xi_{of} = \frac{B_0^2}{8\pi}$. Here B_0 is the field from the Jensen and Cain plus Mead model. In Fig. 4, this field depression is plotted for the particle energy density profile given by Eq. (8), as well as the third order ring current field. It is immediately obvious that while this plasma effect is important, it alone very poorly describes the field deformation in the heart of the ring current region. In fact, as the particle energy density profile is enhanced, the disparity between the two field profiles is also increased. Thus Akasofu's point that the complicated geometry of the magnetosphere must be considered in determining the ring current is clearly born out (Akasofu, 1962).

It also must be pointed out that Eq. (9) does not give the true diamagnetic depression of the field, which is

$$\Delta B_d = - \frac{4\pi \xi_n}{B} \qquad (10)$$

where B is the Jensen and Cain plus Mead plus a self consistent ΔB_d. Such a ΔB_d is also plotted in Fig. 4, and shows an even worse comparison with the 3rd Order field than $\Delta B(1)$. However, it must be pointed out that this expression for diamagnetism neglects all currents in regions external to the cell in which ξ_n is considered.

FIELD DISTORTIONS

Next we investigate the effect of various particle energy density enhancements on the deformation of the field. It should be restated here that these calculations pertain to the sunward side of the magnetosphere only.

In Fig. 5 is plotted the fractional change in field strength at various equatorial distances as a function of K. The fractional change is negative for all distances except 7.0. The field line at 3.0 is on the inner side of the particle distribution maximum, at 3.5 near the maximum ΔB, at 4.25 near the maximum fractional change of the field, and at 7.0, in the region where the ring current enhances the field value. It appears that for our particular distribution of particles, K would have to exceed 500% before a null in the field would exist, and there would be no difficulty in obtaining a self consistent solution to the problem for any K less than this value.

The total field, Jensen and Cain plus Mead plus third order ring current, is shown in Fig. 6 in the region of maximum distortion. Not until slightly more than a 140% particle profile is introduced does a field gradient reversal emerge.

The introduction of larger energy densities of particles does not, at first sight with Fig. 5, produce a strictly proportionately larger field perturbation, at slight variance to the work of Sckopke (1966). He proved that for any particle distribution the field decrease at the center of the earth is given by

$$\frac{\Delta B}{B_0} = -\frac{2\Sigma_p}{3\Sigma_f} \tag{11}$$

where B_0 is the magnetic field intensity at the earth's surface on the magnetic equator, Σ_p is the total energy of the particles, and Σ_f is the total field energy above the earth's surface.

The apparent discrepancy with Sckopke's work is possibly twofold. First, it could be caused by the use of the analytically tractable dipole field model in which the effects of the inclusion of particles are ignored.

Secondly, it could be due to the fact that the total energy content of the particles used is not linear with K. While the particle energy density in each cell at the equator depends directly upon K, it is determined in all the other cells from the relative field values at the cell and the equatorial crossing of the field line through the cell, as well as the energy density value at the equatorial

crossing point, i.e. by the magnetic field configuration. But the magnetic field configuration itself depends upon K. Therefore, the various enhancements of the energy density in each cell are not linearly related to each other. Since the region in which the currents are calculated is limited to within the latitudes $\pm 32°$, the total energy within this region, or sum of ξ_n (cells), will be slightly non-linear with K.

In Fig. 7, ΔB for the third order calculation at the earth is plotted as a function of the total particle energy in the magnetic field. Also shown for comparison is the ΔB of Eq. 11, with $\Sigma_f = 8.37 \times 10^{24}$ ergs and $B_0 = 31{,}000$ gamma, as well as K. Indeed, K is not linear with Σ_p, and neither is ΔB. Therefore it appears that both causes speculated upon produce the apparent non-linearity of Fig. 5 with Sckopke's results. Over most of the range of Σ_p, ΔB is increased over the ΔB of Eq. 11 by about one-third, although the percentage difference slowly increases with Σ_p. In spite of the differences shown here Sckopke's work provides a convenient means of estimating the magnetic effect of any distribution of particles. In fact it appears that the particles are actually more "magnetically efficient" than expected, so for a given Dst a smaller total energy of particles is required.

Field lines have been traced for the ξ_n (140%) particle distribution and appear in Fig. 8. In spite of the rather large energy content of the particles with respect to the field, the field lines are not immensely moved nor distorted.

While the figure shows the Jensen and Cain plus Mead model line at about 4.5 earth radii moved out about a half earth radius, the true quantitative effects of the particles on the field line displacement have not been calculated. These field line traces originate at common points at $\pm 32°$ magnetic latitude, not at the surface of the earth, so they are not applicable to the radial motion of particles due to the violation of the third invariant.

ELECTRIC CURRENT DISTRIBUTIONS

While it may appear as a digression, it is well here to consider the electric current distributions on a magnetic meridian plane from which the ring current fields are calculated. A comparison of two maps of current contours in units of 10^{-3} esu/cm^2-sec. are shown in Fig. 9 for the case K = 70%. The dashed curves are the currents for the first order calculation, the solid curves for the third order.

From the comparison, three features are to be noticed: (1) the positive eastward currents on the inner side of the particle distribution are slightly enhanced. (2) The westward (negative) current contours near the equator on the outer side of the particle distribution are essentially unchanged. (3) The high latitude lobes of the current contours, especially noticeable for the -2×10^{-3} esu/cm^2-sec. contour, are shifted towards the equator.

The third feature is easily explained by looking at the field line traces of Fig. 8. A field line in the model containing the ring current has a smaller

radius of curvature than a field line in only the Jensen and Cain plus Mead model. Since the particle distribution is defined at the equator, independent of the field configuration in which they move, particles with small equatorial pitch angles would have their trajectories shifted towards the equator as they follow the field lines to their mirror points at high latitudes. Therefore, as a result of the particle intensity distribution contours being pulled towards the equator at high latitudes, the current contours would also.

The first and second features have essentially a common explanation, which also clarifies why the higher order ring current fields shown in Fig. 2 and Fig. 3 have smaller magnitudes than the first order in the region near the earth. Consider first the principle term in Eq. (3), $(c/B^2) \cdot B_\theta \cdot (\partial p_n/\partial r) \simeq (c/B) \cdot (\partial p_n/\partial r)$ near the equator, which has a 1/B dependence, since this is the principle diamagnetic effect. One would expect, at first sight, that the currents would be enhanced with the introduction of the self consistent ring current field into the field model, which decreases B. This would be especially true in the region of largest fractional decrease of the field near 4.25 R_E. This fact does occur, causing feature 1, the enhanced eastward current.

However, at larger distances, a competing effect becomes important: that due to the smaller radius of curvature of the lines of force for the model with the ring current. Since p_n is larger than p_s in the second main term of Eq. (2) and Eq. (3) for pitch angle distributions with maximum intensity at 90° pitch angle,

this term always contributes an eastward current, opposite the westward current from the first term, and is inversely proportional to the radius of curvature. (See Hoffman and Bracken, 1965, for a physical explanation of these terms.) Thus the introduction of the ring current field enhances this curvature current. By way of example at 4.2 R_E, Table II contains the partial currents from the two terms in Eq. (2), the first term from diamagnetism in a field configuration with straight field lines, and the second term from the curvature of the field lines. The "diamagnetism" term increases inversely with the field strength, as it should, but the curvature term becomes very important only for the third order calculation. The net westward current is thus essentially unchanged. This again bears out Akasofu's point that the interplay between particles and fields in a self consistent magnetosphere is difficult to analyze (Akasofu, 1962).

Since the eastward current is enhanced, and the westward current remains about the same, each succeeding higher order field becomes slightly smaller inside the particle distribution.

ENERGY DENSITY DISTRIBUTIONS

We finally investigate the ability of the field to contain large densities of particles without the field itself becoming obliterated. In Eq. (1) let $\xi_f = B^2/8\pi$, the final field energy density, and as before $\xi_{of} = B_0^2/8\pi$, and since at the equator $p_n = \xi_n$, the equation becomes

$$\frac{\xi_n}{\xi_{of}} + \frac{\xi_f}{\xi_{of}} = 1 \qquad (12)$$

In Fig. 10 we have plotted the left side of Eq. (12) as a function of ξ_n / ξ_{of} for various distances at the equator. Except for a region on the inner side of the particle belt, the total energy density of particles and fields is larger than the original field energy density.

From the curves at distances in the heart of the belt, 3.5 and 4.25 R_E, there does not appear to be any indication that the total energy could not increase considerably more than is shown as ξ_n / ξ_{of} is further enhanced. It is also to be noted that the total energy density on the outside of the belt is greatly enhanced over the original internal field plus boundary field density. This would cause a relocation of the boundary to larger distances.

Finally it is impressive to consider the ratio of particle energy density to the final field energy density: $\beta = \xi_n / \xi_f$. Several profiles are shown in Fig. 11. One sees that as K is increased, β very rapidly exceeds 1.0 in the region near the heart of the belt. In fact, at a given distance, the value of β is very non-linear with K, as shown in Fig. 12. Referring to Fig. 5, even for a $\beta = 6$ at $R = 4.25$, the fractional field change only reaches 42%.

DISCUSSION

The first point that must be emphasized in a discussion of these results is that they pertain to the steady state for a symmetric ring current.

The fact that particle distributions have been considered which produce β's much larger than one is not necessarily meant to imply that such situations are believed to occur in the magnetosphere. Certainly the maximum particle fluxes allowed will be governed by plasma instabilities and/or the mechanism by which energy is deposited into this region of the magnetosphere (Kennel and Petschek, 1966). However, it has been shown that very large particle energy densities will not themselves provide the limitation by obliterating the field. Therefore, it is required of dynamic mechanisms to quantitatively place the upper limits on β.

Also it has been clearly shown that one must carefully and properly calculate the field from a given particle distribution. Simple estimates of the magnetic effect, such as considering diamagnetism only, can only be assumed to be accurate to a factor of two or worse. In this light, the results presented here pertain only to one particular particle distribution. Other distributions show somewhat different field distortions. Due to the fact that the vector ring current field at any point is an integral over the entire current distribution, the modification of the current distribution in one limited region has serious effects on the field at points outside this region.

The fact that Frank (1967) has measured on the night side a ratio of particle energy density to dipole field energy density in the vicinity of one should not be interpreted as a limit on β of one. The final field configuration, including both

the tail and ring current contributions, must be first calculated in a self consistent manner, or the field must be measured.

Actually the possible ability of the magnetosphere to hold large energy densities of particles relieves one considerably when an explanation is attempted for very large magnetic storms. Chapman and Bartels (1940) provide a list of the most violent storms since 1857, and include a case of $\Delta H > 960\gamma$ at Bombay, and aurora seen there, and several much larger events at Potsdam. Even discounting the possible asymmetric portions of the main phase and the earth's induction, symmetric ring currents must provide field depressions considerably larger than 200 γ at the surface of the earth.

ACKNOWLEDGEMENTS

The authors gratefully acknowledge the assistance and suggestions of many people in the formulation and interpretation of this study, especially Drs. J. C. Cain, G. D. Mead, D. J. Williams, A. Konradi, D. B. Beard, and Mr. L. R. Davis.

TABLE I

Enhancement Factor F	$\frac{\xi_n}{\xi_d}$ (%) K
1.0	40
1.5	60
1.75	70
2.5	100
3.5	140
5.0	200

TABLE II

	Diamagnetism	Curvature	Total
1st Order	-4.36×10^{-3}	$+1.25 \times 10^{-3}$	-3.11×10^{-3}
3rd Order	-5.51×10^{-3}	$+2.48 \times 10^{-3}$	-3.03×10^{-3}

APPENDIX

Notation

a earth radius, centimeters

c speed of light, cm/sec.

B magnetic field, gauss

p_n pressure of the gas normal to the magnetic field

p_s pressure of the gas parallel to the magnetic field

p_m magnetic field pressure or energy density $= B^2/8\pi$

α pitch angle of trapped particle

s distance along a line of force measured from the magnetic equator

r range from the center of the earth

$R_E = r/a$ in earth radii

$\triangle B$ scaler ring current field. At the geomagnetic equator $= B_z$ of Eq. (5).

The subscript "e" indicates that a quantity is being evaluated at the magnetic equator ($s = 0$).

REFERENCES

Akasofu, S.-I., On a self-consistent calculation of the ring current field, J. Geophys. Res., 67, 3617-3618, 1962.

Akasofu, S.-I., The main phase of magnetic storms and the ring current, Space Science Reviews, II, 91-135, 1963.

Akasofu, S.-I., J. C. Cain, and S. Chapman, The magnetic field of a model radiation belt, numerically calculated, J. Geophys. Res., 66, 4013-4026, 1961.

Akasofu, S.-I., and S. Chapman, The ring current, geomagnetic disturbance, and the Van Allen radiation belts, J. Geophys. Res., 66, 1321-1350, 1961.

Cain, J. C., W. E. Daniels, S. J. Hendricks, and D. C. Jensen, An evaluation of the main geomagnetic field, 1940-1962, J. Geophys. Res., 70, 3647-3674, 1965.

Chapman, S. and J. Bartels, Geomagnetism, Oxford, at the Clarendon Press, London, 328, 1940.

Davis, L. R., and J. M. Williamson, Low-energy trapped protons, Space Res., 3, 365-375, 1963.

Dessler, A. J., Discussion of paper by R. L. Arnoldy, R. A. Hoffman, and J. R. Winckler, 'Observations of the Van Allen radiation regions during August and September 1959, Part I', J. Geophys. Res., 65, 3487-3492, 1960.

Frank, L. A., Explorer 12 observations of the temporal variations of low-energy electron intensities in the outer radiation zone during geomagnetic storms, J. Geophys. Res., 71, 4631-4640, 1966.

Frank, L. A., Several observations of low-energy protons and electrons in the earth's magnetosphere with OGO 3, J. Geophys. Res., 72, 1905-1916, 1967a.

Frank, L. A., On the extraterrestrial ring current during geomagnetic storms, U. of Iowa preprint 67-9, 1967b.

Hendricks, S. J., and J. C. Cain, Magnetic field data for trapped-particle evaluations, J. Geophys. Res., 71, 346-347, 1966.

Hoffman, R. A., and P. A. Bracken, Magnetic effects of the quiet-time proton belt, J. Geophys. Res., 70, 3541-3556, 1965.

Kennel, C. F., and H. E. Petschek, Limit on stably trapped particle fluxes, J. Geophys. Res., 71, 1 - 28, 1966.

Mead, G. D., Deformation of the geomagnetic field by the solar wind, J. Geophys. Res., 69, 1181-1195, 1964.

Parker, E. N., Newtonian development of the dynamical properties of ionized gases of low density, Phys. Rev., 107, 924-933, 1957.

Sckopke, N., A general relation between the energy of trapped particles and the disturbance field near the earth, J. Geophys. Res., 71, 3125-3130, 1966.

Stratton, J. A., Electromagnetic Theory, McGraw-Hill Book Company, New York, 1941.

Van Allen, J. A., Some general aspects of geomagnetically trapped radiation, Radiation Trapped in the Earth's Magnetic Field, ed. by B. M. McCormac, D. Reidel Pub. Co., Dordrecht-Holland, 1966.

Williams, D. J., and G. D. Mead, Nightside magnetosphere configuration as obtained from trapped electrons at 1100 kilometers, J. Geophys. Res., 70, 3017-3029, 1965.

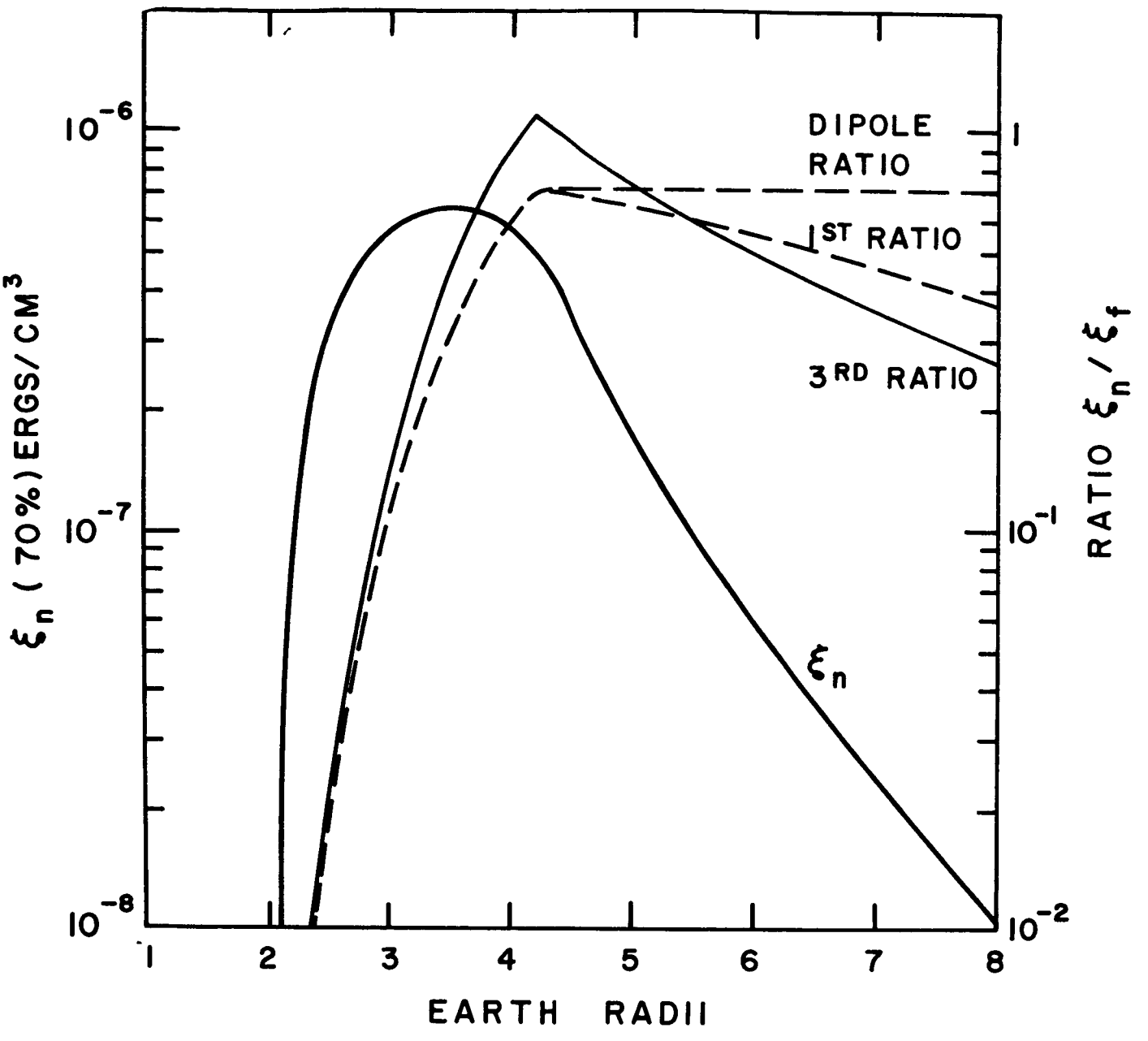

Figure 1. Equatorial energy density profile ξ_n (70%). Ratios of this energy density profile to (1) the energy density of the geomagnetic dipole ("Dipole Ratio"), displaying the constant ratio beyond 4.272 R_E, (2) to the energy density of the Jensen and Cain plus Mead field (1st Ratio); and (3) to the energy density of the Jensen and Cain plus Mead plus 3rd order ring current field (3rd Ratio).

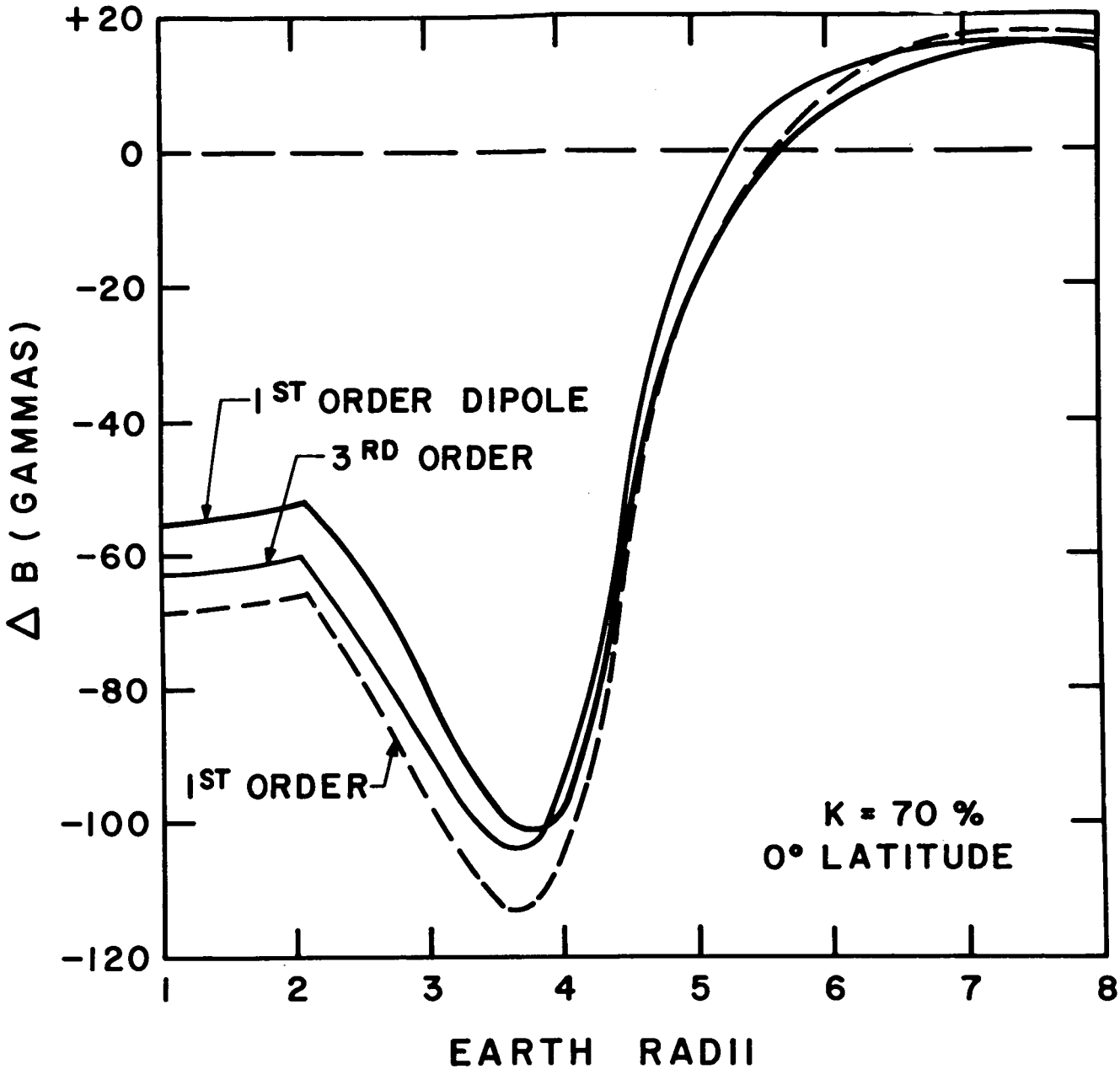

Figure 2. First and third order ring current fields as a function of distance at the equator, and the first order field calculated in the dipole model of the earth's field for K = 70%.

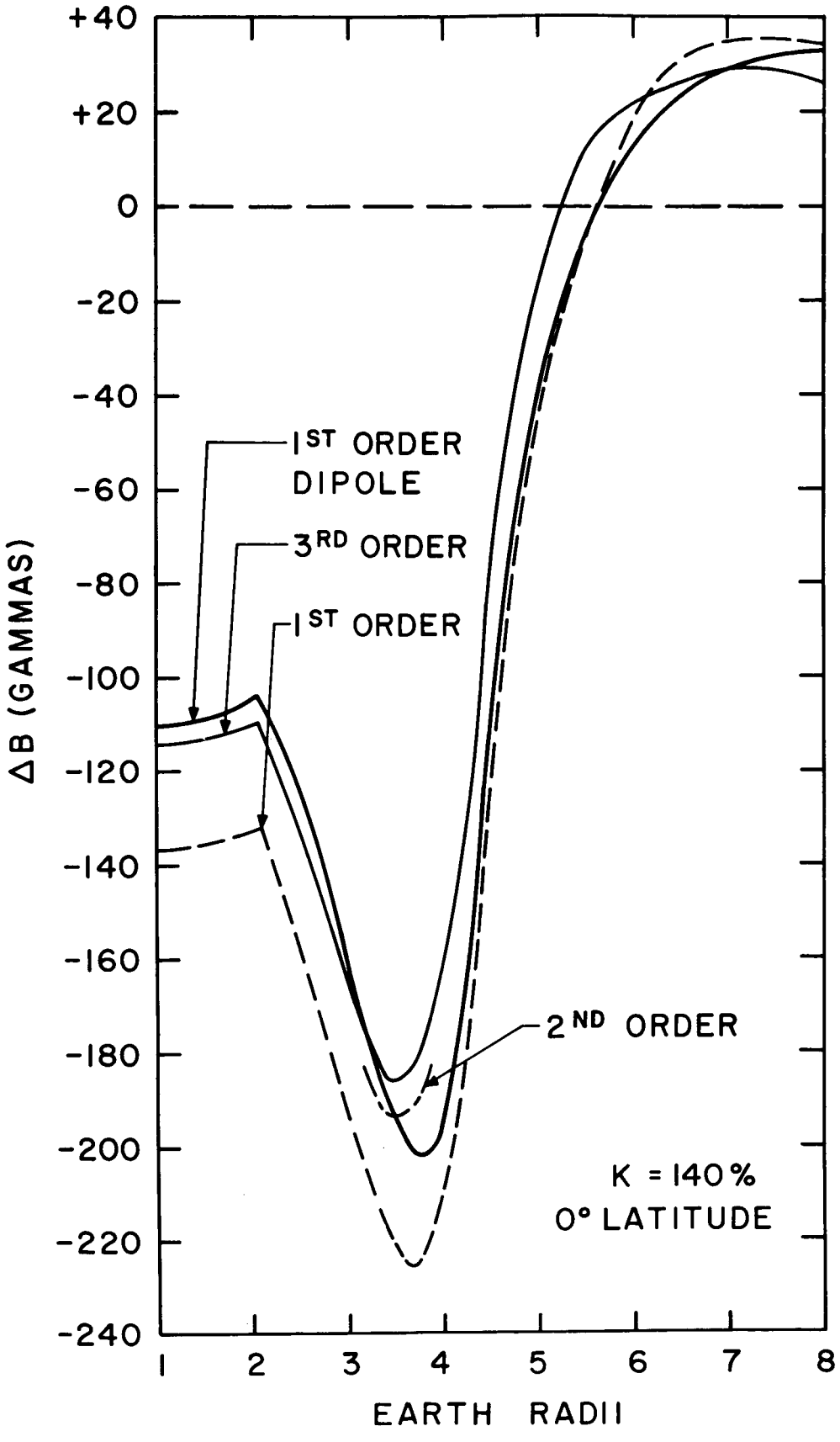

Figure 3. Same as Figure 2 for K = 140%. Also indicated is the 2nd Order calculation in the region of maximum ΔB.

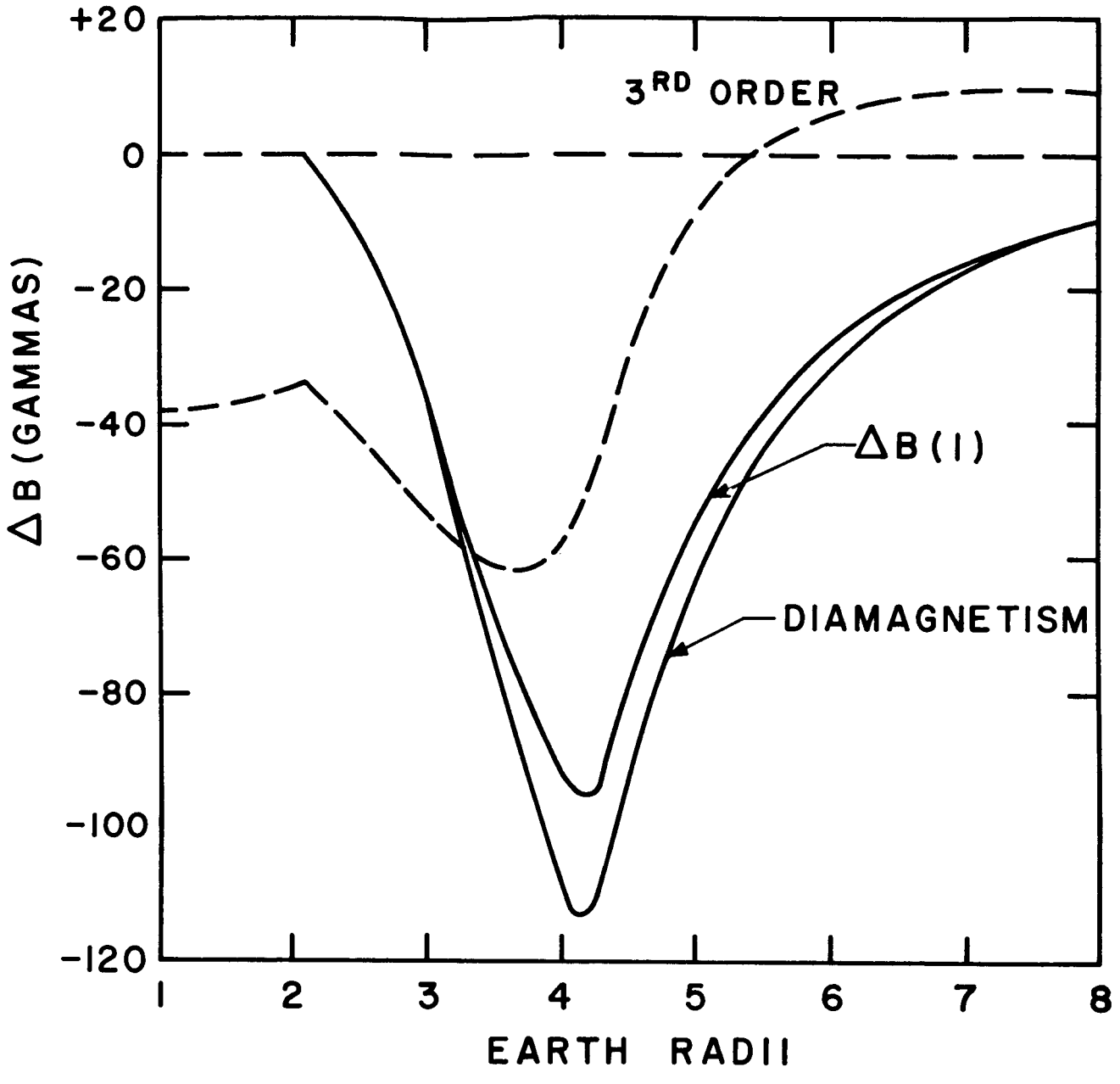

Figure 4. Comparison of the ring current field calculated from (1) all current sources (3rd Order), (2) Eq. (9), ΔB (1), (3) only diamagnetism, (Diamagnetism).

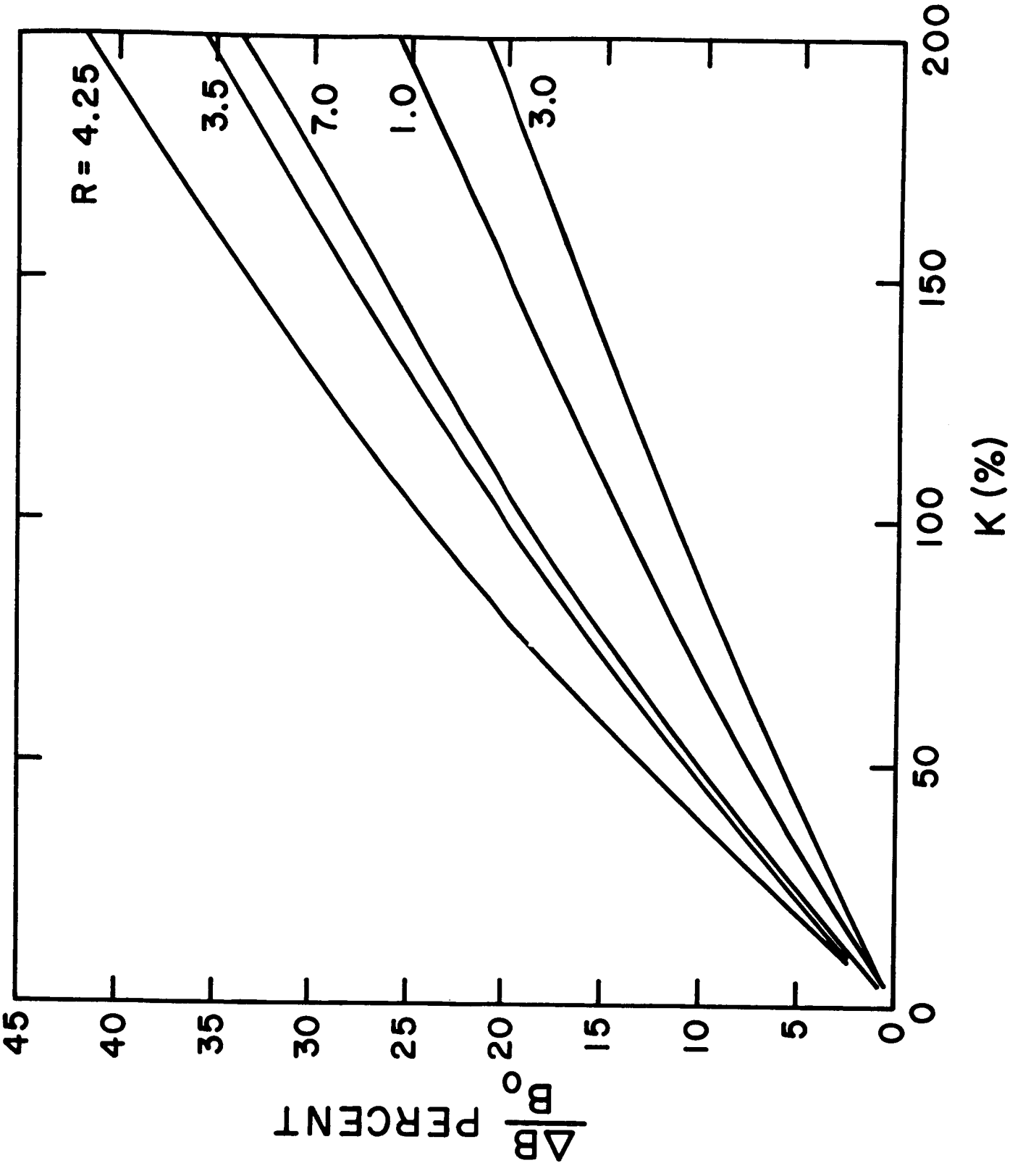

Figure 5. Fractional change in field strength at various equatorial distances as a function of K. The fractional change is negative for all values of R except 7, for which it is positive. B_0 is the Jensen and Cain plus Mead field. The curve of $R_E = 1$ is multiplied by 20.

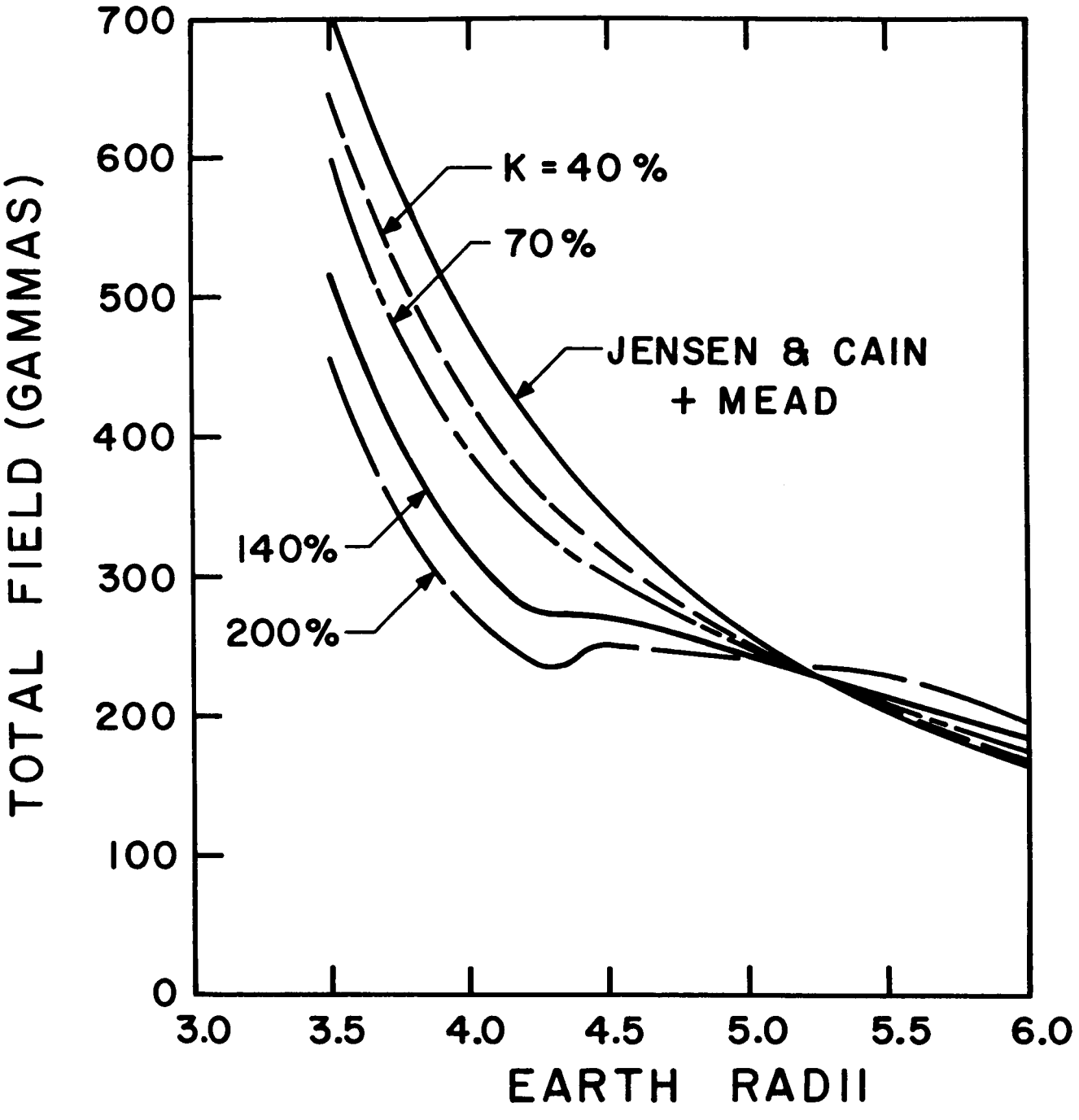

Figure 6. Total magnetic field, Jensen and Cain plus Mead plus third order ring current in the region of maximum distortion for various enhancements of the energy density profile.

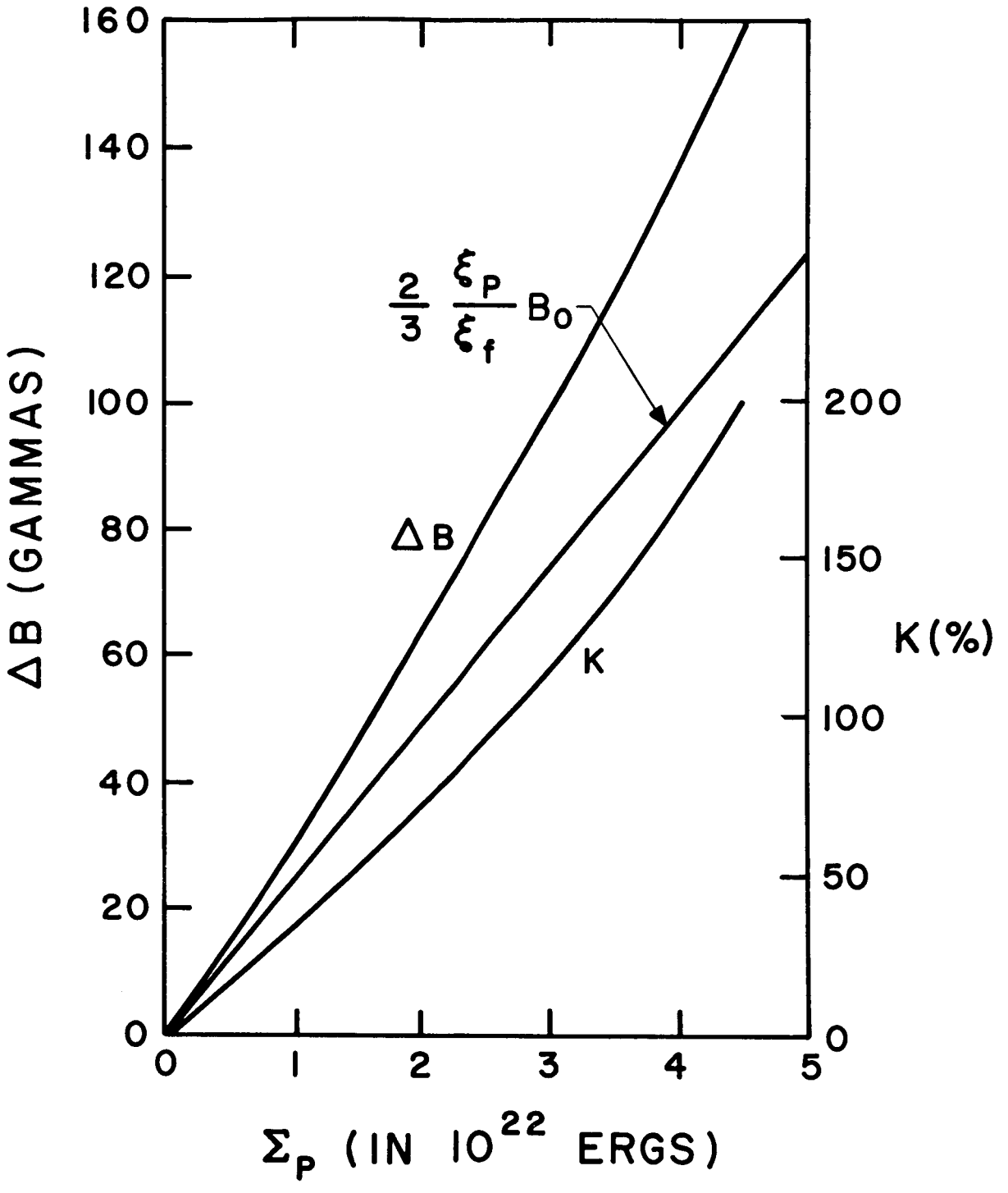

Figure 7. ΔB for the third order calculation at the earth as a function of the total particle energy in the magnetic field. Also shown is ΔB from Eq. (11) as well as K.

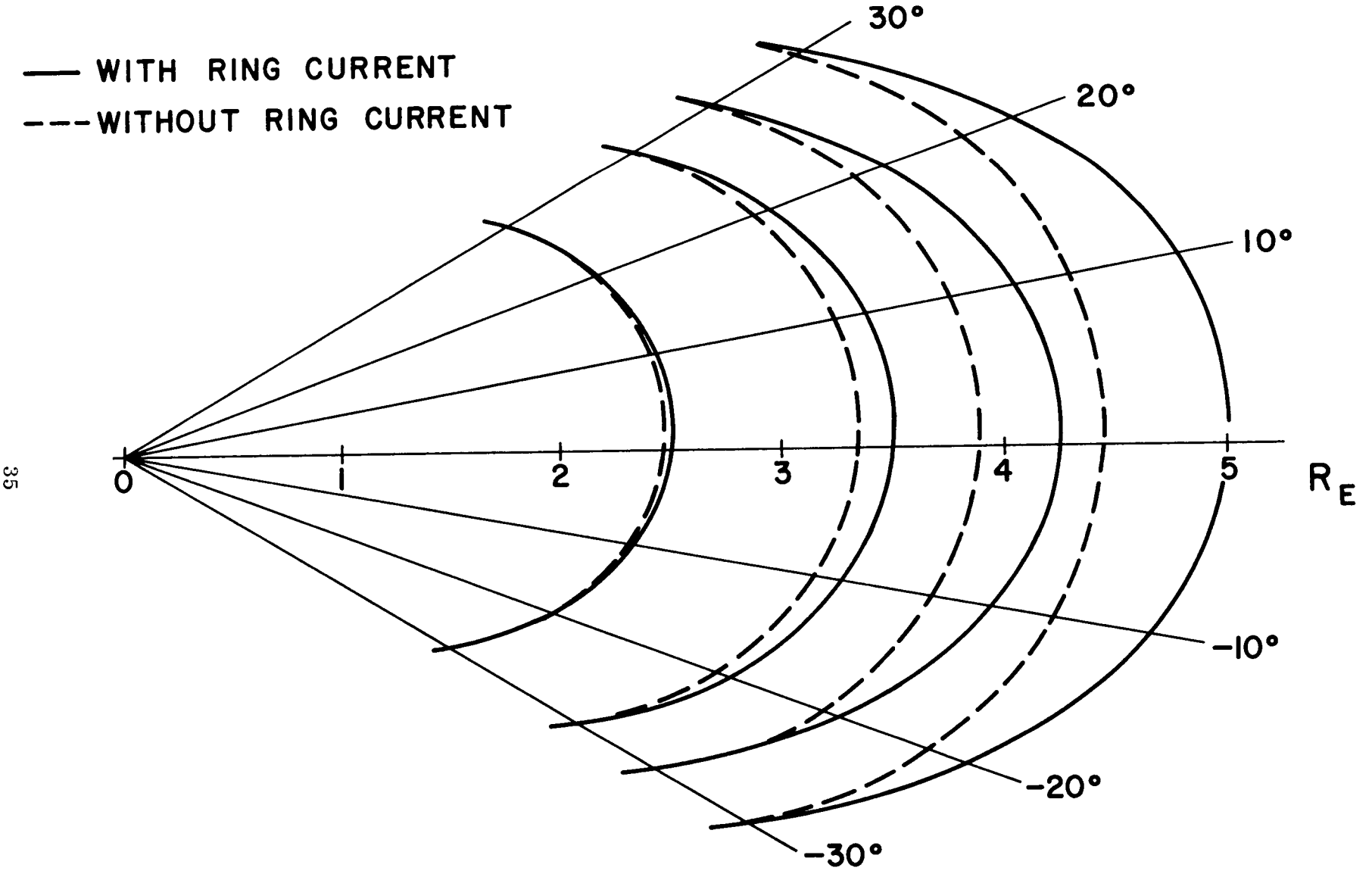

Figure 8. Field line traces for ξ_n (140%).

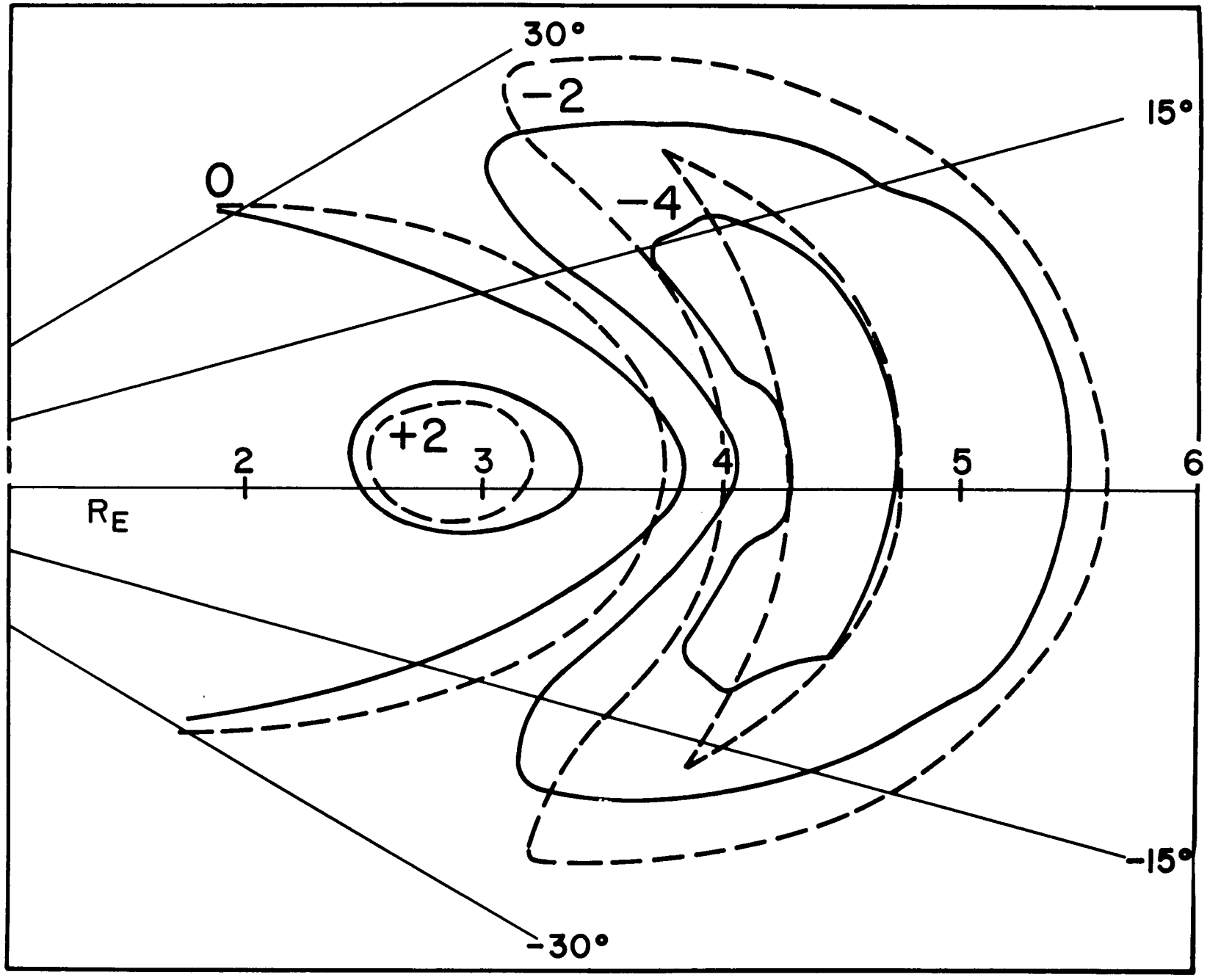

Figure 9. Electric current contours in units of 10^{-3} esu/cm^2-sec. for K = 70%. The dashed curves are the currents for the first order calculations, the solid curves for the third order. Eastward currents are positive, westward currents are negative.

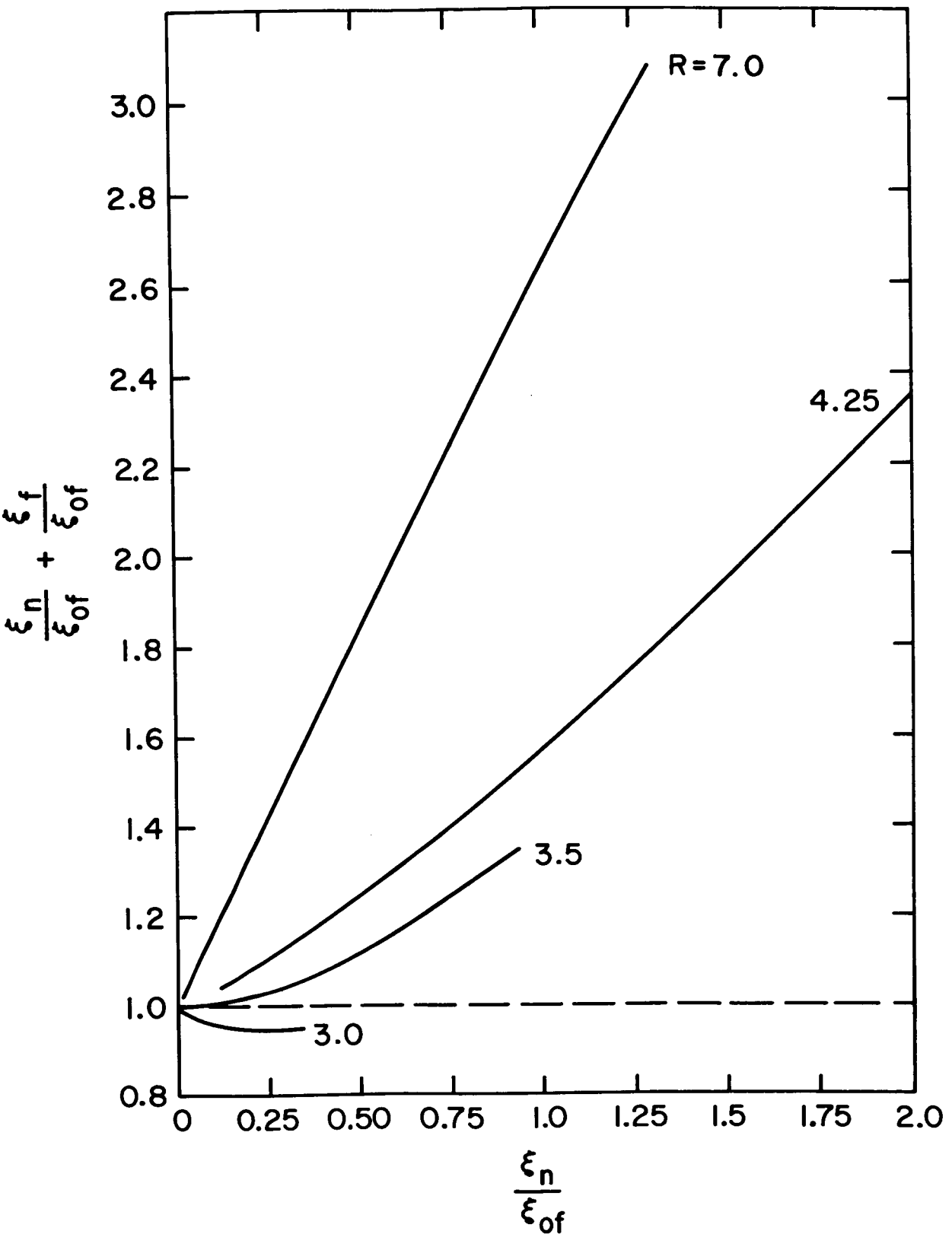

Figure 10. The left side of Eq. (12) as a function of ξ_n/ξ_{of} for various distances at the equator.

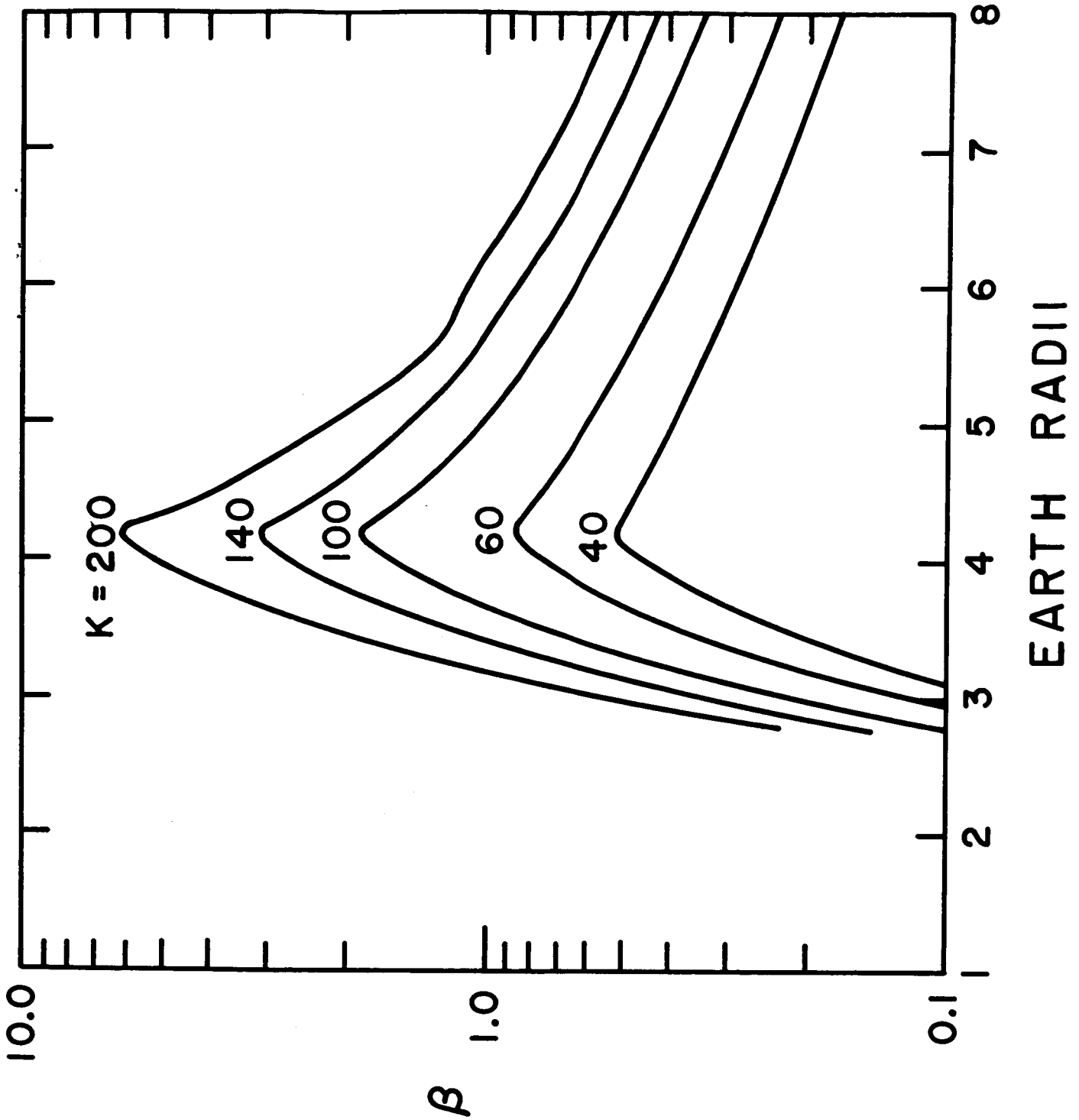

Figure 11. Profiles of $\beta = \xi_n/\xi_f$ for various values of K.

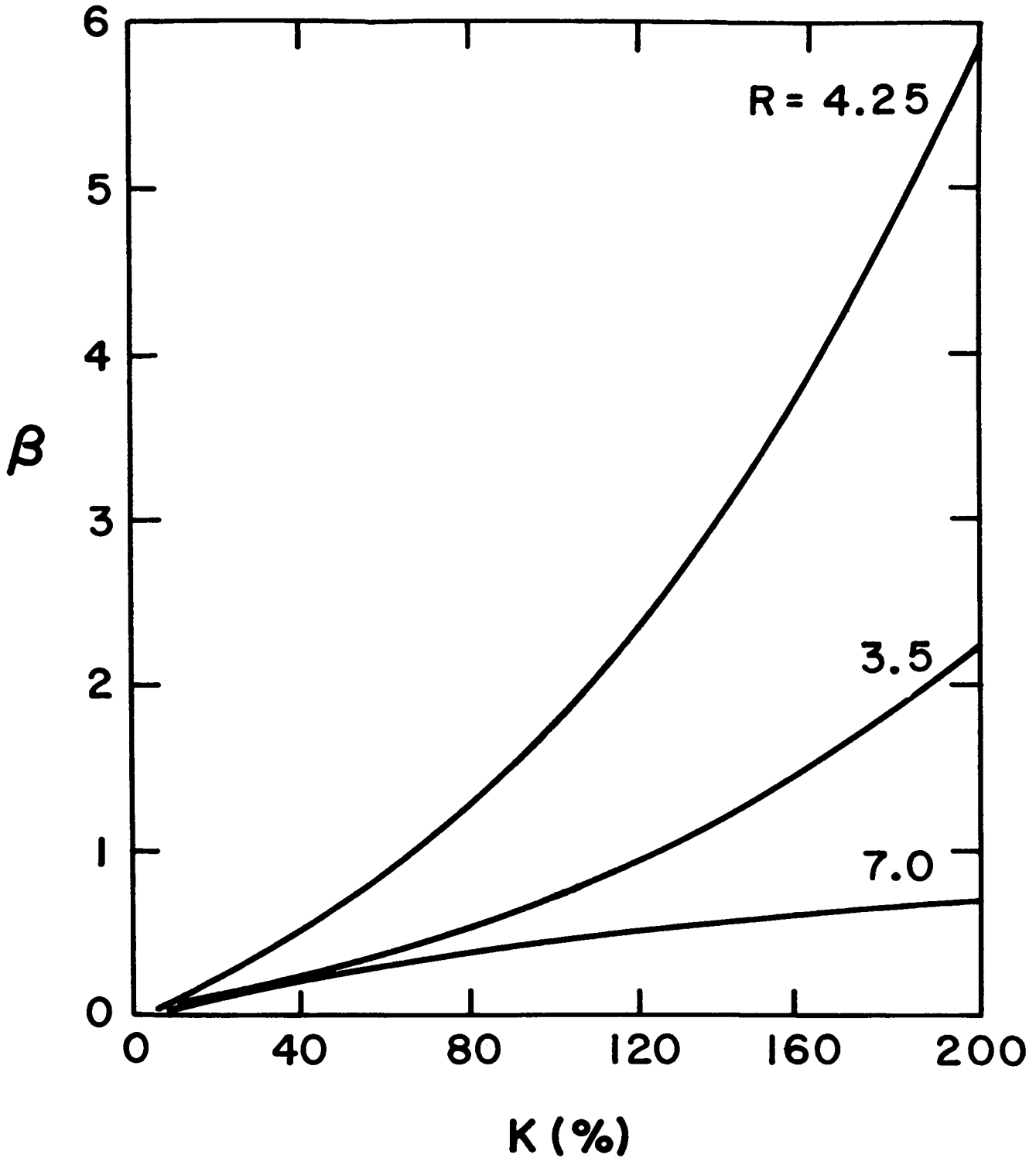

Figure 12. β as a function of K for several equatorial distances.